1986ApJ...309..846L

THE ASTROPHYSICAL JOURNAL, 309:846–857, 1986 October 15
© 1986. The American Astronomical Society. All rights reserved. Printed in U.S.A.

ON THE TIDAL INTERACTION BETWEEN PROTOPLANETS AND THE PROTOPLANETARY DISK. III. ORBITAL MIGRATION OF PROTOPLANETS[1]

D. N. C. LIN AND JOHN PAPALOIZOU
Canadian Institute for Theoretical Astrophysics, University of Toronto; Lick Observatory, Board of Studies in Astronomy and Astrophysics, University of California, Santa Cruz; and School of Mathematical Sciences, Queen Mary College, London, England

Received 1985 November 22; accepted 1986 April 8

ABSTRACT

We continue our investigation of the tidal interaction between a protoplanet and a gaseous protoplanetary disk. We consider the dynamical evolution of the disk and the orbital migration of the protoplanet in a self-consistent manner. We show that the orbital migration of a protoplanet does not suppress the tendency for tidal truncation in the vicinity of its orbit. If the necessary condition for tidal truncation is satisfied, the protoplanet induces a tidal feedback mechanism that regulates the rate of angular momentum transfer between the protoplanet and the disk. Significant orbital migration can only occur on the viscous evolution time scale of the disk.

Subject headings: planets: formation — stars: formation

I. INTRODUCTION

Giant planets in the solar system contain mainly hydrogen and therefore must have been formed in a gas-rich environment. If the gas they contain was accreted from a protoplanetary disk, their mass, chemical composition, and orbital position may have been determined by the details of the dynamical interaction between their progenitors and the disk (Lin and Papaloizou 1985). For example, strong tidal interaction between a protoplanet and the disk may induce gap formation in the disk and thereby inhibit the protoplanet's mass growth by accretion. Using a simple impulse approximation, Lin and Papaloizou (1979*a*, *b*) showed that the rate of angular momentum transport from the protoplanet to a cold, tidally truncated disk is given by

$$\dot{H}_T = \mathrm{sign}\,(\Delta_0)\,\frac{8}{27}\left(\frac{M_p}{M}\right)^2 \Sigma_n R_p^4\,\omega^2 \left(\frac{R_p}{|\Delta_0|}\right)^3 , \qquad (1)$$

where M is the mass of the Sun, M_p, R_p, and ω are the mass, orbital radius, and orbital angular frequency of the protoplanet, Σ_n is the nearby disk's surface density, $\Delta_0 \equiv R_0 - R_p$, and R_0 is the radius of the disk's edge. A similar result can also be obtained by summing over a series of pointlike contributions from the Lindblad resonances in the disk (Goldreich and Tremaine 1980, 1982). For a gaseous disk in which the thermal pressure supports a moderate thickness in the direction normal to the plane of the disk, the effects of sonic propagation of the tidal disturbance and the modification of resonance conditions associated with the pressure gradient in the radial direction need to be considered. In the linear approximation (Papaloizou and Lin 1984), we found that

$$\dot{H}_T \le \mathrm{sign}\,(\Delta_0) f \left(\frac{M_p}{M}\right)^2 \Sigma_n R_p^4\,\omega^2 \left(\frac{R_p}{H_\infty}\right)^3 , \qquad (2)$$

where the constant $f \approx 0.23$. To obtain equation (2), we used a polytropic equation of state with polytropic index 1.5. We also adopted a particular Σ_n profile with its radial scale height comparable to the thickness of the disk H_∞.

Where, in the disk, is this angular momentum deposited? In principle, it may not be deposited in the close vicinity of the protoplanet's orbit if the effective viscosity ν is very small and the sound speed is relatively large. However, when a protoplanet is sufficiently massive so that its Roche radius $R_R \equiv (M_p/M)^{1/3} R_p \approx |\Delta_0| \gtrsim H_\infty$, the tidal disturbance may induce local nonlinear shock dissipation and hence angular momentum exchange. Thus, it may be reasonable to assume that most of the exchange occurs in the close vicinity of R_0. In general, a necessary condition for the tidal truncation of a viscous disk is

$$\dot{H}_T \gtrsim \dot{H}_\nu \approx 3\pi\nu\Sigma_n R_0^2\,\omega , \qquad (3)$$

where $\dot{H}_\nu$ is the viscous angular momentum transfer rate in the disk, or equivalently,

$$\frac{M_p}{M} \gtrsim \left(\frac{40\nu}{R_p^2\,\omega}\right)^{1/2} \left(\frac{H_\infty}{R_p}\right)^{3/2} . \qquad (4)$$

Note that if $\nu \approx \alpha H_\infty c_s$, where α is a dimensionless parameter (Shakura and Sunyaev 1973), equation (4) implies that the necessary condition for tidal truncation is $R_R/R_p \gtrsim (40\alpha)^{1/6}(H_\infty/R_p)^{5/6}$. In the protoplanetary disk, $\alpha \approx 10^{-2}$ (Lin and Papaloizou 1985; Ruden and Lin 1986), so that the above criterion is only satisfied when $R_R \gtrsim H_\infty$. Using a self-consistent, nonlinear, two-dimensional hydrodynamic calculation, Lin and Papaloizou (1986) showed that equation (1) provides a reasonably good approximation for $\dot{H}_T$ for cases with $H_\infty/R_p \lesssim 0.1$ and verified the tidal truncation condition given by equation (4). Thus, when a gap first forms, it is likely that $|\Delta_0| \approx R_R \gtrsim H_\infty$, so that the exchange of angular momentum is local.

The truncation condition (4) is derived on the basis that R_p is constant. However, angular momentum exchange between the disk and the protoplanet may cause secular orbital evolution of the protoplanet (Goldreich and Tremaine 1980) such that

$$M_p\,\omega R_p \dot{R}_p/2 = -\dot{H}_T . \qquad (5)$$

[1] *Lick Observatory Bulletin*, No. 1045.

© American Astronomical Society • Provided by the NASA Astrophysics Data System

1986ApJ...309..846L

Hourigan and Ward (1984) postulated that unless the time scale for orbital migration across the gap, $\tau_\Delta \approx |\Delta_0|/\dot{R}_p$ is longer than the characteristic time scale associated with gap formation $\tau_{\rm gap}$, tidal truncation of the disk may be prohibited by the orbital migration of the protoplanet. They deduced that the necessary condition for a protoplanet to induce tidal truncation is $M_p \gtrsim 0.2\pi\Sigma_n H_\infty^2$ if $H_\infty \approx 0.1 R_p$. The implications of their results, in the case of the protoplanetary disk, are: (1) tidal truncation may not have occurred in the protoplanetary disk at all, and (2) both high- and low-mass protoplanets must have undergone substantial orbital migration. In order to verify their conjectures, Hourigan and Ward (1984) carried out an idealized analysis in which they considered the response of the disk to the tidal influence of a moving protoplanet. However, their results depend on an arbitrarily imposed surface density variation. If this is omitted, the physical implication of their equation (14) is a general tendency for a migrating protoplanet to induce a local surface density variation which acts to reverse the direction of migration. Thus, the effect of orbital migration on the truncation condition remains uncertain and unsettled.

In § II we utilize the heuristic approach adopted by Hourigan and Ward to examine various characteristic time scales and show that the orbital migration may not be able to prevent gap formation. We verify these arguments using a self-consistent numerical scheme, to solve equations that reduce to those of Hourigan and Ward when viscosity is zero. With this scheme, we calculate the evolution of the disk as well as that of the protoplanet's orbit. In § III, we briefly describe the basic equations and the numerical method, and in § IV we present the results that indicate that orbital migration does not prohibit tidal truncation.

After the protoplanet opens up a gap, it may still tidally interact with the disk and thereby undergo orbital migration. At the same time, the disk is evolving viscously. It is also of interest to compare the magnitude of the characteristic orbital migration time scale $\tau_R \approx R_p/\dot{R}_p$ with that of the disk's viscous evolution time scale, $\tau_\nu \approx R_p^2/\nu$, which is determined by the effective magnitude of viscosity in the disk. In the protoplanetary disk, turbulence generated by convection provides $\tau_\nu \approx 10^5$–10^6 yr (Lin and Papaloizou 1980; Lin 1981; Lin and Bodenheimer 1982). If $\tau_R \gtrsim \tau_\nu$, the protoplanet's orbital migration may be coupled to the viscous diffusion of the gas. Since the disk is depleted on the viscous time scale, there would be little postformation orbital migration. In this case, there is some physical basis to the phenomenological models in which the disk surface density distribution is estimated by augmenting the mass of giant planets and spreading it between their present orbits (Cameron 1962). The absence of significant orbital migration for the prototerrestrial planets is also implicitly assumed in the deduction of the disk temperature distribution from the condensation temperature of various main constituents in terrestrial planets (Lewis 1972, 1974). However, if $\tau_R < \tau_\nu$, the protoplanets may undergo considerable postformation migration. Rapidly migrating protoplanets can result in the evolution of the disk being essentially determined by tidal transport of angular momentum, via the protogiant planets, rather than viscous transport of angular momentum, via intrinsic turbulent motion. Thus, if $\tau_\nu > \tau_R$, we must construct a new series of models for the structure and evolution of the protoplanetary disk. In order to resolve this important issue, we present some results on posttruncation orbital evolution in § V. The implication of these results in the context of the formation of the solar system is presented in § VI.

II. CHARACTERISTIC TIME SCALES

From equations (1) and (5), we derive the characteristic orbital evolution time scale across the protoplanetary disk

$$\tau_R \approx \frac{M_p \omega R_p^2}{\dot{H}_T} \approx \left(\frac{M}{M_p}\right)\left(\frac{M}{\delta\Sigma_n R_p^2}\right)\left(\frac{|\Delta_0|}{R_p}\right)^3\left(\frac{1}{\omega}\right), \tag{6}$$

where $\delta\Sigma_n$ is the difference between the disk surface density at $\sim|\Delta_0|$ interior and exterior to the protoplanet. For an arbitrary power-law initial surface density distribution, $\Sigma_n \propto R^k$, $\delta\Sigma_n \approx k|\Delta_0|\Sigma_n/R_p$. If we assume $|\Delta_0| \approx H_\infty$ and ignore tidally induced changes in the surface density distribution, we find

$$\tau_R \approx \left(\frac{M}{M_p}\right)\left(\frac{M}{k\Sigma_n R_p^2}\right)\left(\frac{H_\infty}{R_p}\right)^2 \frac{1}{\omega}. \tag{7}$$

Applying typical values of disk mass ($\pi\Sigma_n R_p^2 \approx 0.02$–$0.1\ M_\odot$), $H_\infty(\sim 0.05$–$0.1 R_p)$, and k of order unity, we would find $\tau_R \approx 10^3$–10^4 yr for a Jovian-mass protogiant planet and $\tau_R \gtrsim 10^6$ yr for all prototerrestrial planets. Note that, since the characteristic orbital evolution time scale $\tau_R \gg \omega^{-1}$, the constant forcing frequency assumption in evaluating $\dot{H}_T$ is still valid. Under the same assumptions, the time scale for orbital migration across the gap is $\tau_\Delta \approx \Delta_0/\dot{R}_p \approx \tau_R \Delta_0/R_p \lesssim 0.1\tau_R$.

If the angular momentum transfer due to viscous stress is ignored, the continuity equation for the disk gas is reduced to

$$2\pi\dot{\Sigma}_n \approx -\frac{1}{R}\frac{\partial}{\partial R}\left(\frac{2}{\Omega R}\frac{\partial \dot{H}_T}{\partial R}\right). \tag{8}$$

At a distance $|\Delta_0| \approx H_\infty$ from the protoplanet, the characteristic time scale for gap formation is

$$\tau_{\rm gap} \approx \frac{\Sigma_n}{\dot{\Sigma}_n} \approx \left(\frac{M}{M_p}\right)^2\left(\frac{H_\infty}{R_p}\right)^5 \frac{1}{\omega}. \tag{9}$$

In comparison with τ_Δ, we find $\tau_{\rm gap}/\tau_\Delta \approx (\Sigma R_p^2/M_p)(H_\infty/R_p)^2$. Hourigan and Ward's conjecture is based on the idea that if $\tau_{\rm gap}/\tau_\Delta \gtrsim 1$, tidal truncation of the disk may be prevented. However, their scenario, by assuming a fixed Σ_n profile, inadequately describes the disk response to the protoplanet's tide. We propose that provided the disk can modify the local surface density gradient on a time scale $\tau_{\rm grad}$ short compared with τ_Δ, the protoplanet can evolve into a quasi-equilibrium configuration such that $\dot{H}_T$ from either side of the protoplanet's orbit is delicately balanced and $\dot{R}_p$ is substantially reduced from that induced by the original surface density distribution. The relevant time scale for modifying the original local surface density gradient is $\tau_{\rm grad} \approx (H_\infty/R_p)\tau_{\rm gap}$, so that $\tau_{\rm grad}/\tau_\Delta \approx (\Sigma_n R_p^2/M_p)(H_\infty/R_p)^3$. Provided $R_R \gtrsim H_\infty$, $\tau_{\rm grad}/\tau_\Delta \lesssim \Sigma_n R_p^2/M \lesssim 0.1$ Thus, the orbital migration may not prohibit tidal truncation of the disk.

For protoplanets with $R_R \lesssim H_\infty$ that are embedded in the disk, we can no longer use the vertical averaging approximation to estimate the magnitude of $\dot{H}_T$. In this case, the tidal phenomenon must be investigated with a three-dimensional analysis. For example, even for a geometrically thin disk, the pressure gradient in the direction normal to the plane of the disk can strongly modify the resonance conditions. Even if we were to ignore these subtleties and estimate τ_R, $\tau_{\rm grad}$, and τ_Δ, we would find the orbital migration proceeds at a much slower rate for low-mass than for high-mass protoplanets. Thus, we speculate there is little orbital migration for low-mass prototerrestrial planets due to tidal interaction with the disk.

© American Astronomical Society • Provided by the NASA Astrophysics Data System

1986ApJ...309..846L

Note that if $R_R \lesssim H_\infty$, the growth time scale, during the gas accretion phase, is

$$\tau_m \approx M_p/\dot{M}_p \approx M_p/(c_s \rho R_B^2) \qquad (10)$$

where ρ ($\approx \Sigma_n/2H_\infty$) is the disk density and $R_B \approx GM_p/c_s^2$ is the Bondi radius. In this case, gas accretion is not strongly affected by the protoplanet's tidal effect and $\tau_m \approx (M/M_p)(M/\Sigma_n R_p^2)(H_\infty/R_p)^4\omega^{-1} \ll \tau_\Delta < \tau_R$. This comparison implies that once a protogiant planet enters the gas accretion phase, it would accrete from the disk at essentially the same location until R_R becomes comparable to H_∞. Thereafter, the protoplanet accretes essentially all the gas streaming past its orbit, so that the accretion rate becomes $\sim 2\pi\Sigma_n U_r R_p$, where U_r is the radial velocity of the disk gas and $U_r \approx -1.5\nu/R_p$ in the limit of a steady state. When $R_R \gtrsim H_\infty$ but the necessary condition is not satisfied, $\tau_m \approx \tau_\Delta < \tau_R$, so that there may be a small amount of orbital migration. However, when the necessary condition in equation (4) is satisfied, $\tau_m \gtrsim \tau_{\rm gap}$ for almost all cases. Thus, we may investigate the tidal truncation process while neglecting the mass increase in the protoplanet.

III. THE EVOLUTION EQUATIONS AND THE NUMERICAL METHOD

The tidal effect of protoplanet-disk interaction can be incorporated into the viscous evolution calculation of the disk. Averaging over all azimuthal phases and integrating over the direction normal to the plane of the disk, the ϕ-component of the equation of motion becomes

$$\Sigma_n U_r \frac{dR^2\Omega}{dR} = \frac{1}{R}\frac{\partial}{\partial R}\left(\nu\Sigma_n R^3 \frac{d\Omega}{dR}\right) + \Sigma_n \Lambda , \qquad (11)$$

where Λ is the injection rate of angular momentum per unit mass by tidal interaction with the protoplanet. Near the orbit of the protoplanet, the small departure from Keplerian rotation does not significantly affect the local angular momentum transfer rate, provided the Rayleigh stability criterion is satisfied. Since we are primarily interested in the orbital migration of protoplanets which can truncate the disk, we only consider the case where the Rayleigh's stability criterion is satisfied and adopt a Keplerian approximation such that $\Omega = (GM/R^3)^{1/2}$. Then equation (11) becomes

$$\Sigma_n R U_r = 2\Sigma_n \Lambda \frac{R^{3/2}}{(GM)^{1/2}} - 3R^{1/2}\frac{\partial}{\partial R}\nu\Sigma_n R^{1/2} . \qquad (12)$$

Using equation (12) to eliminate $\Sigma_n U_r R$, the continuity equation gives

$$\frac{\partial \Sigma_n}{\partial t} = -\frac{1}{R}\frac{\partial}{\partial R}\Sigma_n U_r R = \frac{1}{R}\frac{\partial}{\partial R}\left[3R^{1/2}\frac{\partial}{\partial R}\left(\nu\Sigma_n R^{1/2}\right) - \frac{2\Lambda\Sigma_n R^{3/2}}{(GM)^{1/2}}\right] . \qquad (13)$$

To calculate the evolution of a disk with an embedded protoplanet, we need to specify the functional form of Λ which depends on the distribution of tidal dissipation in the disk. If ν is relatively large, this dissipation is concentrated in the vicinity of the protoplanet's orbit (Papaloizou and Lin 1984). If ν is relatively small, nonlinear phenomena, such as shocks, may cause the dissipation to be concentrated near the edge, as discussed above (Lin and Papaloizou 1986). Thus, it is probably adequate to utilize the results derived from both the impulse approximation and resonant interaction calculation such that

$$\Lambda = \text{sign}\,(R - R_p)\,\frac{fq^2 GM}{2R}\left(\frac{R}{|\Delta_p|}\right)^4 . \qquad (14)$$

In equation (14), $q \equiv M_p/M$ and f is a constant of order unity. In accordance with equation (2), $|\Delta_p|$ is taken to be the maximum of H_∞ or $|R - R_p|$. This prescription provides a simple and reasonably good approximation for the results derived from summing over Lindblad resonances (Goldreich and Tremaine 1980; Hourigan and Ward 1984). Note that this modified prescription does not prevent a discontinuous change of sign for Λ at R_p. For a smooth Σ profile, discontinuities in Λ can cause a gap to start to form under any conditions, since it provides a much larger magnitude for the second term than the first term on the right-hand side of equation (13). But such a discontinuity is unphysical, since the resonances have finite width and thermal effects can delocalize the resonances at R_p. In order to assure Λ is continuous, we adopt an ad hoc approximation in which sign $(R - R_p)$ is replaced with $(R - R_p)/H_\infty$ for $|R - R_p| \leq H_\infty$.

By total angular momentum conservation, the protoplanet's orbit must also evolve such that

$$\frac{M_p}{2}\left(\frac{GM}{R_p}\right)^{1/2}\frac{dR_p}{dt} = -\frac{dH_T}{dt} = -2\pi\int_{R_{\rm in}}^{R_{\rm out}} \Lambda R \Sigma_n \, dR , \quad (15)$$

where dH_T/dt is the total rate of tidal angular momentum transfer and $R_{\rm in}$ and $R_{\rm out}$ are the inner and outer boundaries of the disk. Equations (13)–(15) together describe the disk and protoplanetary orbit evolution. They can be solved for arbitrary viscosity laws. For example, according to both the self-consistent convective model and the standard α prescription,

$$\nu = \nu_0(\Sigma_n/\Sigma_0)^2 \qquad (16)$$

in the solar disk (Lin and Papaloizou 1980; Lin 1981; Lin and Papaloizou 1985). For computational convenience, we can introduce a set of dimensionless variables such that $\tau = t\nu_0/R_0^2$, $\Sigma = \Sigma_n/\Sigma_0$, $r = R/R_0$, $r_o = R_{\rm out}/R_0$, $r_i = R_{\rm in}/R_0$, and $r_p = R_p/R_0$, where R_0 is some suitably chosen radial scaling length, for example, the initial radius of the outermost radius of the disk. With these variables, equations (13) and (15) become

$$\frac{\partial\Sigma}{\partial\tau} = \frac{3}{r}\frac{\partial}{\partial r}\left[r^{1/2}\frac{\partial(r^{1/2}\Sigma^3)}{\partial r} - \text{sign}\,(r - r_p)\Sigma r^{1/2} A\left(\frac{r}{\delta_p}\right)^4\right] \quad (17)$$

and

$$\dot{r}_p \equiv \frac{dr_p}{d\tau} = -2BAr_p^{1/2}\int_{r_i}^{r_o}\Sigma\left(\frac{r}{\delta_p}\right)^4 \text{sign}\,(r - r_p)\, dr , \quad (18)$$

where $\delta_p \equiv \Delta_p/R_0$, $A \equiv (GMR_0)^{1/2}q^2 f/(3\nu_0)$ is a measure of the strength of the tidal effects in comparison to viscosity and $B \equiv 3\pi\Sigma_0 R_0^2/M_p$ is a measure of the mass ratio of the disk to the protoplanet. In order to open up a gap in the disk, the two terms in the brackets in equation (17) must become comparable. In a disk with $\Sigma \approx 1$, the condition for forming a gap, with a scale length comparable to H_∞, is $R_0/H_\infty \lesssim A(R_0/H_\infty)^4$, or $A \lesssim (H_\infty/R_0)^3$. If A becomes larger, the gap becomes wider than H_∞. In the cases to be presented below, we limit the minimum values of δ_p to be $h_0 \equiv H_\infty/R_0$. For computational convenience, in each case, one value of h_0 is chosen for the entire disk and it is not changed during the calculation. This procedure may lead to an underestimate of h_0 in the outer regions and an overestimate in the inner region of the disk.

Equations (17) ahd (18) can be solved numerically with standard explicit finite difference techniques (Richtmyer and Morton 1967). In various applications, we choose different prescriptions for the numerical grid structure and boundary conditions. For example, in § IV, where we examine gap formation

© American Astronomical Society • Provided by the NASA Astrophysics Data System

1986ApJ...309..846L

for very low mass protoplanets, the relevant characteristic length scale and time scale are relatively small. In order to provide a good spatial resolution, we set up 200 grid points equally spaced between $r = 0.5$ and $r = 0.9$ with $r_p = 0.701$ initially. Since we are only interested in the dynamics for $\sim\tau_{\rm gap}$, we take Σ at the inner and outer boundaries to be constants during these short intervals of time. In § V, we are interested in the long-term evolution of relatively massive protoplanets in a viscous evolving disk. In this case, relatively coarse spatial resolution is adequate, and we set up 1000 grid points equally spaced between $r = 0$ and $r = 20$. Although, for all cases, we adopt the convention that there is no disk material at large r initially, the extended range in r is used to satisfy the freely expanding outer boundary condition. For the inner boundary condition, we adopt the standard constant $\dot{M}$ assumption (Bath and Pringle 1981), so that the Sun accretes from the disk at a rate which is determined by the viscous evolution of the disk at large distances from the Sun. For the viscosity prescription (16), constant $\dot{M}$ implies constant Σ.

IV. GAP FORMATION

With the above formulation, we can verify the heuristic arguments in § II with detailed numerical computation. In Figure 1, we plot the surface density distribution at four epochs for various initial Σ distributions. In all cases, we place the protoplanet initially at $r_p = 0.701$. In order to evaluate the response of the disk under a variety of conditions, we examine four sets of values for A, B, and h_0 ($\equiv H_\infty/R_0$) (see Table 1), with the same initial surface density distribution, $\Sigma(\tau = 0) = 1 - r$ (cases I–IV are plotted in Figs. 1a–1d). Although these values of A, B, and h_0 are relevant for tidal interaction between prototerrestrial planets and a massive protoplanetary disk, they are chosen primarily on the ground that $\tau_\Delta \lesssim \tau_{\rm gap}$ in every case. According to Hourigan and Ward (1984), a gap may not be formed in any of these cases despite the fact that $A \gtrsim h_0^3$ in all cases. Note that in all these cases $\tau_\Delta \gtrsim \tau_{\rm grad}$ and the heuristic arguments suggest that the necessary and sufficient conditions for gap formation are satisfied.

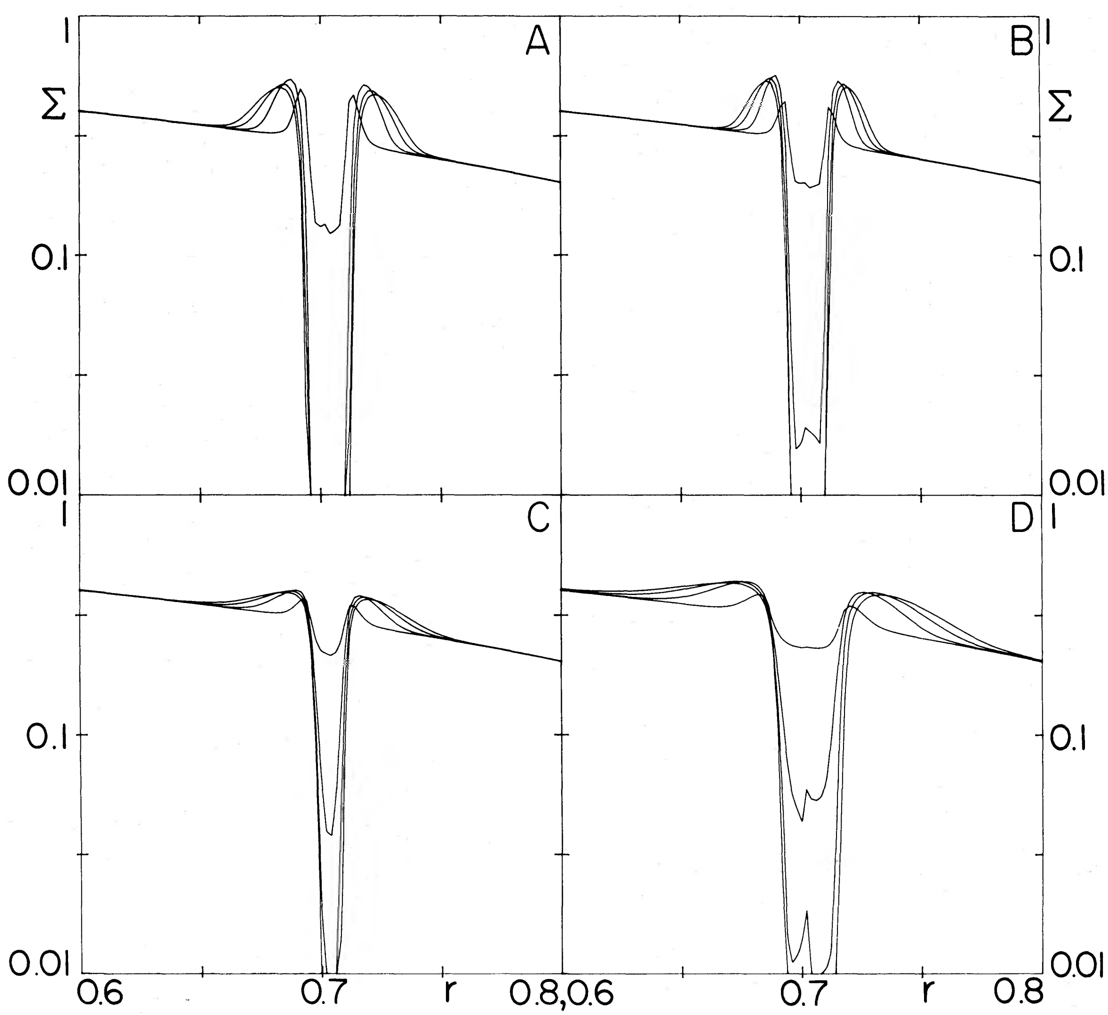

FIG. 1.—Gap formation induced by protoplanetary-disk tidal interaction. In (a)–(d), four sets of A, B, and h_0 are taken (cases I to IV) for the same initial condition ($\Sigma = 1 - r$). The four Σ plots for (a) case I are plotted for $\tau = 2.3 \times 10^{-6}$, 1.6×10^{-5}, 3×10^{-5}, 4.5×10^{-5}. For (b) case II they are 1.2×10^{-6}, 8.2×10^{-6}, 1.5×10^{-5}, 2.2×10^{-5}. For (c) case III they are 9.3×10^{-6}, 6.5×10^{-5}, 1.2×10^{-4}, 1.8×10^{-4}. For (d) case IV they are 2.3×10^{-5}, 1.6×10^{-4}, 3×10^{-4}, 4.5×10^{-4}.

© American Astronomical Society • Provided by the NASA Astrophysics Data System

1986ApJ...309..846L

TABLE 1

SUMMARY OF MODEL PARAMETERS

Model	A	B	h_0	$\Sigma(t=0)$ $(r_i\text{–}r_o)$	r_p	Figure
I	10^{-5}	10^5	10^{-2}	$1 - r(0.5\text{–}0.9)$	0.701	1*a*
II	10^{-5}	10^6	10^{-2}	$1 - r(0.5\text{–}0.9)$	0.701	1*b*
III	10^{-6}	10^5	10^{-2}	$1 - r(0.5\text{–}0.9)$	0.701	1*c*
IIIa	10^{-6}	10^5	2×10^{-2}	$1 - r(0.5\text{–}0.9)$	0.701	...
IV	10^{-5}	10^5	2×10^{-2}	$1 - r(0.5\text{–}0.9)$	0.701	1*d*
IVa	10^{-5}	10^6	2×10^{-2}	$1 - r(0.5\text{–}0.9)$	0.701	...
V	0	10^6	...	1(0–1)	1	2*a*, 3*a*(a)
VI	0	10^6	...	1(1–2)	1	2*c*, 3*b*(a)
VII	10^{-3}	20	0.05	1(0–1)	1	2*b*, 3*a*(b)
VIII	10^{-3}	20	0.05	1(1–2)	1	2*d*, 3*b*(b)
IX	10^{-3}	20	0.05	1(0–1)	04, 0.6, 0.7, 0.8	4, 5
X	10^{-3}	0.1, 1, 0.5, 20, 80	0.05	1(0–1)	0.7	6
XI	10^{-3}	5	0.05	1(0–1)	0.8, 0.7, 0.6	7*a*
XII	10^{-3}	80	0.05	1(0–1)	0.8, 0.7, 0.6	7*b*
XIII	$5 \times 10^{-3}, 10^{-3}, 2 \times 10^{-4}$	1	0.05	1(0–1)	0.7	8*a*
XIV	$10^{-2}, 10^{-3}, 10^{-4}$	5	0.05	1(0–1)	0.7	8*b*
XV	$5 \times 10^{-3}, 10^{-3}, 2 \times 10^{-4}$	20	0.05	1(0–1)	0.7	8*c*
XVI	$5 \times 10^{-3}, 10^{-3}, 2 \times 10^{-4}$	1, 5, 25	0.05	1(0–1)	0.7	8*d*

In case I, the protoplanet temporarily moved outward. Using the initial Σ distribution in equation (18), we find that $\dot{r}_p \approx 0.1BA(r_p/h_0)^3$ is positive and attains a magnitude of 10^4. However, the magnitude of $\dot{r}_p$ decreases rapidly, and gap formation proceeds immediately. After $\Delta\tau \approx 2.3 \times 10^{-6}$, the surface density in the neighborhood of r_p has decreased by more than a factor of 3. In dimensionless units, $\tau'_{\rm gap} = \tau_{\rm gap} v_0/R_0^2 = h_0^5/3A \approx 3 \times 10^{-6}$ for case I. For a typical disk model, this time scale is comparable to the dynamical time scale. The disk material which is initially located inside the gap is transferred to the surrounding regions under the protoplanet's tidal torque. However, due to the transitory outward movement of the protoplanet, the magnitude of Σ increases slightly more for the region $r > r_p$ than for $r < r_p$ so that the gradient in Σ is reduced. As the protoplanet approaches the Σ enhancement just outside r_p, the tidal interaction becomes more intense than that between the protoplanet and the Σ enhancement immediately interior to r_p. Consequently, $\dot{r}_p$ changes sign in order to adjust to a quasi-tidal equilibrium in which the angular momentum transfer rate from both sides of r_p is delicately balanced. This flow pattern indicates that the disk's response to the protoplanet's tide can provide a self-regulating influence on the evolution of both the protoplanet's orbit and the disk's Σ distribution. After the initial transitory adjustment, the protoplanetary orbit evolves on a viscous time scale.

In case II, although the mass of the disk is 10 times larger than M_p, gap formation proceeds on nearly the same time scale as in case I. Thus, we conclude that there is not an "inertial limit" as proposed by Hourigan and Ward (1984). The larger values of B in case II induce a larger magnitude for $\dot{r}_p$ initially. However, as in case I, the disk self-regulates its evolution as well as $\dot{r}_p$, so that eventually the self-consistent evolution of the system occurs on a viscous time scale. In case III, the smaller magnitude of A makes the condition for gap formation marginal, and the evolution time scale is considerably longer than case I. We have computed an additional case (IIIa) in which the same values of A and B are used as case III and $h_0 = 0.02$. In that case, $A \lesssim (h_0/r_p)^3$ and gap formation is inhibited. In case IV, a relatively large magnitude for h_0 causes $\tau_{\rm grad}$ to become comparable to τ_Δ. Nevertheless, a gap is formed on the time scale of $\sim 10^{-4}$. Again, we computed another case (IVa) with the same values of A and h_0 as case IV and $B = 10^6$, so that $\tau_{\rm grad} \gtrsim \tau_\Delta$. Gap formation is also inhibited.

In addition to these models, we considered cases with a variety of initial Σ distribution. In each case, the tidally induced self-regulating process modulates the disk structure and the protoplanet's orbital evolution. The long-term evolution of the disk structure and protoplanet's orbit is independent of the initial surface density distribution. For computational convenience, we adopt a standard initial condition, for all but one set of models below, that the disk have an initial unit surface density ($\Sigma = 1$) distribution between $r = 0$ and $r = 1$.

V. LONG-TERM EVOLUTION OF THE DISK AND THE PROTOPLANET'S ORBIT

Our numerical scheme can be used to study the orbital evolution of a protogiant planet. We first make some estimate of the relevant range of the magnitudes of A and B for protogiant planets in a protoplanetary disk. By adopting the assumption that the chemical composition of the original protoplanetary disk was similar to that of the Sun today, and that most of the volatile materials in the disk were not accreted onto the planets and satellites, a lower limit of the disk's mass may be determined by augmenting the mass of the planets to account for the missing constituents (Cameron 1962). The mass obtained this way is $\sim 2\%$ of the present mass of the Sun. Thus, for a Jovian-mass protoplanet inside a minimum mass disk, B is of order 10. According to the self-consistent convective accretion disk model (Lin and Papaloizou 1980), $\nu \approx 10^{-5}\Omega R_0^2$, so that A is of order 10^{-3}. Based on these estimates, we consider various numerical models within $10^{-2} \geq A \geq 10^{-4}$ and $80 \geq B \geq 0.1$. We ignore changes in A and B associated with the accretion of disk gas by the protoplanet.

a) Protoplanet Initially Located at the Disk's Boundary

We first compute the evolution of a freely expanding disk by setting $A = 0$. The results obtained from this model calculation can be compared with those obtained for a disk which is evolving under the tidal influence of a protoplanet and used to delineate the importance of the tidal effect on the evolution of

© American Astronomical Society • Provided by the NASA Astrophysics Data System

1986ApJ...309..846L

the disk. In Figure 2A, we plot the surface density distribution of a freely evolving disk at five epochs with the initial conditions $\Sigma = 1$ for $0 \leq r \leq 1$ (case V). Under the action of viscous transport, the outer boundary of the disk expands (see curve *a* in Fig. 3*a*) while the surface density over most regions of the disk decreases. Since the magnitude of the viscosity is proportional to Σ^2, the rate of surface density decrease is reduced and the magnitude of τ_v is increased during the course of evolution. We also compute a freely expanding disk with $\Sigma = 1$ at $1 \leq r \leq 2$ and $\Sigma = 0$ elsewhere initially (case VI, Fig. 2*c*). In this case, the inner boundary moves towards the protosun (curve *a* in Fig. 3*b*). Despite the fact that the inner boundary of case VI is initially at the same location as the outer boundary of case V, the inward expansion of the disk's inner boundary, in case VI, proceeds at a rate 10 times faster than that which corresponds to the outward expansion of the outer boundary in case V.

We now compare the evolution of a freely expanding disk with the evolution of the disk under the influence of a protoplanet. In case VII, we adopt $A = 10^{-3}$, $B = 20$, and the standard initial condition that $\Sigma = 1$ for $0 \leq r \leq 1$, and place the protoplanet at the outer edge of the disk, i.e., it has an initial orbital radius $r_p = 1$ (Fig. 2*b*). For case VIII, similar values of A and B are applied to the initial condition that $\Sigma = 1$ for $1 \leq r \leq 2$ and $r_p = 1$ (Fig. 2*d*). In both cases, the presence of the protoplanet has minor influence on the evolution over most regions of the disk. The protoplanet's tide removes sufficient angular momentum from the disk that the evolution of the outer boundary is slower in Figure 2*b*. Since the protoplanet must absorb angular momentum from the disk, its orbit expands (curve *b* in Fig. 3*a*). The dimensionless characteristic time scale for the protoplanetary orbital migration, τ_R ($\approx r_p/[dr_p/d\tau]$ or $M_p \omega R_0^2/[dH_T/d\tau]$ as in eq. [3]) is relatively short initially, and it rapidly increases to a magnitude which is comparable to the viscous time scale. The disk's outer boundary is denoted by curve *c*. On a time scale comparable to $\tau_R \approx h_0^3/AB\Sigma \approx 10^{-2}$, the magnitude of δ_p increases to $\gtrsim h_0$. Thereafter, the rate of the protoplanet's orbital migration, $dr_p/d\tau \propto \Sigma/\delta_p^3$, is reduced until τ_R becomes comparable to τ_v. The magnitude of δ_p cannot increase indefinitely. For sufficiently large δ_p, $dH_v/dt \gtrsim |dH_T/dt|$ at the outer boundary of the disk, the outer edge of the disk expands faster than the orbit of the protoplanet and thereby reduces δ_p. Eventually, a critical distance is maintained between the protoplanet and the outer edge of the disk such that the magnitude of dH_v/dt at the outer edge of the disk slightly exceeds that of $|dH_T/dt|$. Thereafter, the protoplanet's orbital migration is coordinated with the expansion of the disk's outer edge. Since the rate of expansion of the outer edge is determined by the rate of viscous transport of angular momentum throughout the disk, the expansion time scale is comparable to τ_v for the entire disk. Thus, τ_R is also comparable to τ_v. In the present series of numerical computations, δ_p increases to a value of order unity after about one diffusion time scale, whereupon τ_R is reduced to $\sim 0.1/AB\Sigma \approx$ 10–100.

Similarly, in case VII, where a protoplanet is initially located interior to the disk's inner edge, at least initially, the tidal transfer causes the protoplanet to evolve faster than the inner boundary of the analogous freely evolving disk (Fig. 2*d* and 3*b*). Quantitatively, $\tau_R \approx 10^{-2}$ initially as in the previous case.

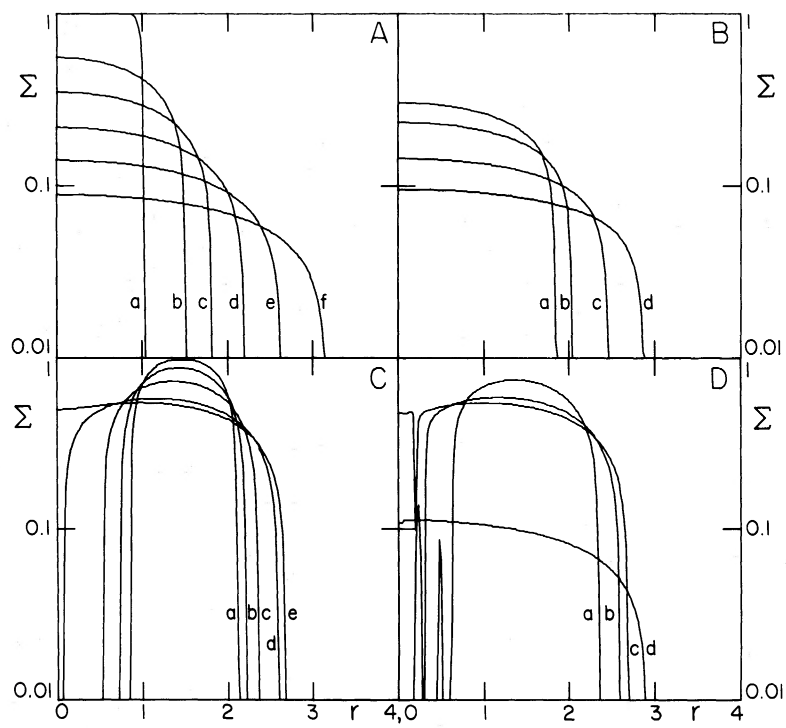

FIG. 2.—Evolution of a disk with or without an external protoplanet. In (*a*) and (*b*) at $\tau = 0$, $\Sigma = 1$ for $r \leq 1$; in (*c*) and (*d*) $\Sigma = 1$ for $1 \leq r \leq 2$ and $\Sigma(t = 0) = 0$ elsewhere. In (*g*) (case V) and (*c*) (case VI), the disk expands freely in the absence of any protoplanet's tidal influence. In (*a*) the curves *a–f* are Σ plots for $\tau = 2 \times 10^{-4}$, 0.1, 0.42, 1.6, 5.6, and 20.3; in (*c*) the curves *a–e* represent $\tau = 3.6 \times 10^{-3}$, 1.2×10^{-2}, 3.5×10^{-2}, 0.113, and 0.158. In (*b*) a protoplanet is placed at $r_p = 1$ initially (case VII). The curves *a–d* are Σ plots for $\tau = 0.66$, 1.4, 5.6, and 17.8. The values of A, B, and h_0 are 10^{-3}, 20, and 0.05. The same values of A, B, h_0, and initial r_p are used for (*d*) (case XIII) so that the protoplanet is initially located at the inner boundary of the disk. The four curves are for $\tau = 3.3 \times 10^{-2}$, 0.11, 0.166, and 10. Note that the presence of the protoplanet does not strongly influence the surface density distribution of the disk at each stage of the evolution.

© American Astronomical Society • Provided by the NASA Astrophysics Data System

1986ApJ...309..846L

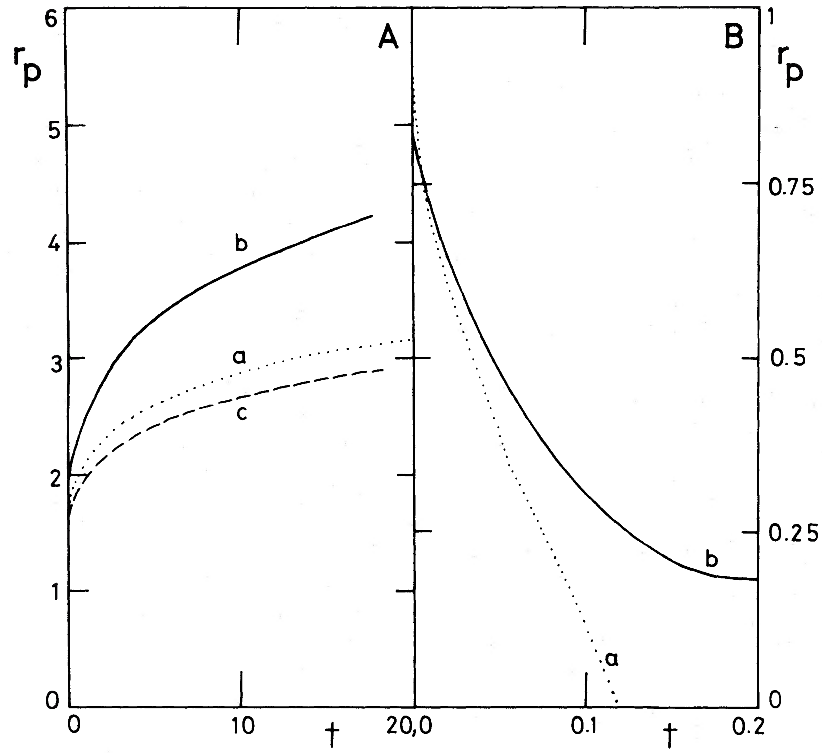

FIG. 3.—Long-term evolution of the disk's boundaries and protoplanet's orbit. At $t = 0$, $\Sigma = 1$ for (*a*) $r \leq 1$ and (*b*) $1 \leq r \leq 2$. Elsewhere $\Sigma = 0$. In (*a*) the location of the outer boundary of a freely expanding disk is plotted in the dotted curve *a* (case V). The dashed curve *c* shows the evolution of the disk's outer boundary subject to an external protoplanet which is initially located at $r_p = 1$, with $A = 10^{-3}$, $B = 20$, and $h_0 = 0.05$. The solid curve *b* shows the protoplanet's orbital evolution. In the dotted curve *a* shows the evolution of the inner boundary of a freely expanding ring with the above-specified initial Σ distribution (case VI). The solid curve *b* represents the orbital evolution of a protoplanet in cases XIII. The protoplanet is initially located at the inner boundary of the disk, i.e.,$r_p = 1$, and the values of *A*, *B*, and h_0 in cases XIII are identical to those in case XII.

In our prescription, we keep $h_0 = 0.05$ so that the limit value of δ_p/r_p increases as the protoplanet evolves toward the origin. At sufficiently small r_p, the tidal effect becomes less effective. Under the dominant action of viscous stress in the disk, the protoplanet penetrates the tidal barrier (Fig. 2*d*). Thereafter, the disk's surface density distribution becomes approximately symmetric in the immediate vicinity of the protoplanet's orbit such that $dr_p/d\tau$ is essentially reduced to zero. We have also examined some additional cases with different values of *A* and *B*. In these cases, although the rate of evolution depends on the magnitude of *A* and *B*, the overall dynamical properties are essentially identical to those found in cases VII and VIII.

b) *The Standard Models with* $A = 10^{-3}$, $B = 20$, *and* $r_p = 0.4$, 0.6, 0.7, *and* 0.8

It is of interest to examine the protoplanet's orbital migration under a wide variety of initial conditions. For this purpose, we adopt a set of arbitrarily chosen values of A (10^{-3}) and B (20) and four initial protoplanetary orbital radii. In Figures 4*a*, 4*b*, and 4*c* we plot the evolution of the surface density distribution with initial $r_p = 0.6$, 0.7, and 0.8 (cases IXb, IXc, and IXd) respectively. These results indicate that, in all cases, the protoplanet opens up a gap in the disk shortly after the onset of the calculation. In doing so, the protoplanet's orbit and the disk in the close vicinity of the protoplanet evolve rapidly. The time scale for the gap opening is $\tau_{\rm gap} \approx \Sigma/(\partial\Sigma/\partial\tau) \approx (h_0/r_p)^5/A \approx 10^{-2}$. In Figures 5*a* and 5*b*, we plot r_p and $dr_p/d\tau$ for initial $r_p = 0.4$ (case IXa) and the above three cases as curves *b*, *d*, *f*, and *h* respectively. After the initial transitory stage, the disk surface density distribution adjusts continually with the protoplanet's orbital position such that the angular momentum transferred from the inner region of the disk to the protoplanet is approximately balanced by that transferred from the protoplanet to the outer region of the disk. Subsequently, the protoplanet's orbital evolution occurs on a viscous diffusion time scale. In Figure 5, we compare the protoplanet's orbital evolution with that of a typical fluid element, which is initially located at 0.4, 0.6, 0.7, and 0.8, in a freely viscously evolving disk (see curves *a*, *c*, *e*, and *g*). For $r_p \gtrsim 0.2$, there is little difference between the magnitude of $dr_p/d\tau$ for the four cases and that of the corresponding fluid elements in a freely expanding disk, i.e., the magnitude of τ_R is comparable to τ_ν, rather than $(h_0/r_p)^3/AB\Sigma$, which is or order 10^{-2}. In case IXa, τ_R is much larger than τ_ν for $r_p \lesssim 0.2$ because, the limiting values of δ_p/r_p decreases with r_p.

The comparison of these four cases indicates that the protoplanet's orbital evolution is very sensitive to the location of the protoplanet with respect to the mass distribution of the disk. If a protoplanet is located in the inner region of the disk, it would evolve toward the protosun on a viscous diffusion time scale. If a protoplanet is located in the outer region of the disk, it would generally migrate outward on somewhat longer time scales. There is an intermediate critical radius where the protoplanet migrates outward at first and then inward (curve *f*). This evolutionary pattern is very similar to that of the complimentary fluid element (curve *e*). The initial outward migration is caused by the "absorption" of angular momentum from the inner parts of the disk. As the inner region of the disk is depleted, the

© American Astronomical Society • Provided by the NASA Astrophysics Data System

1986ApJ...309..846L

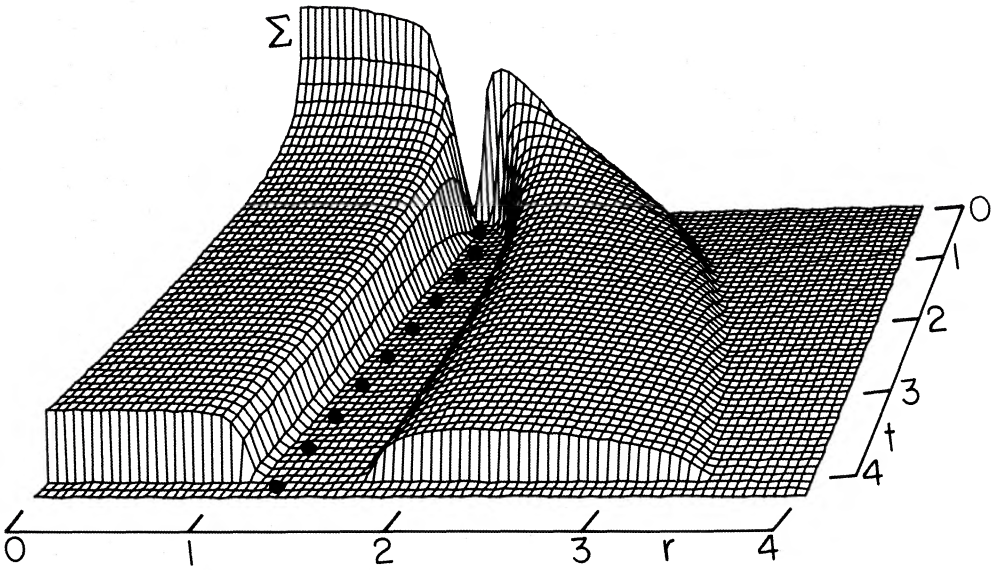

FIG. 4a

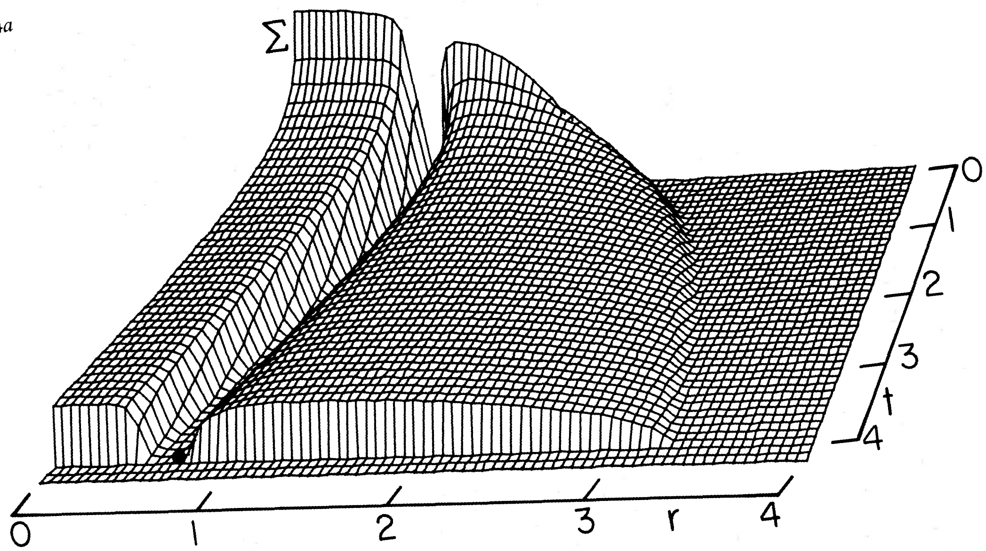

FIG. 4b

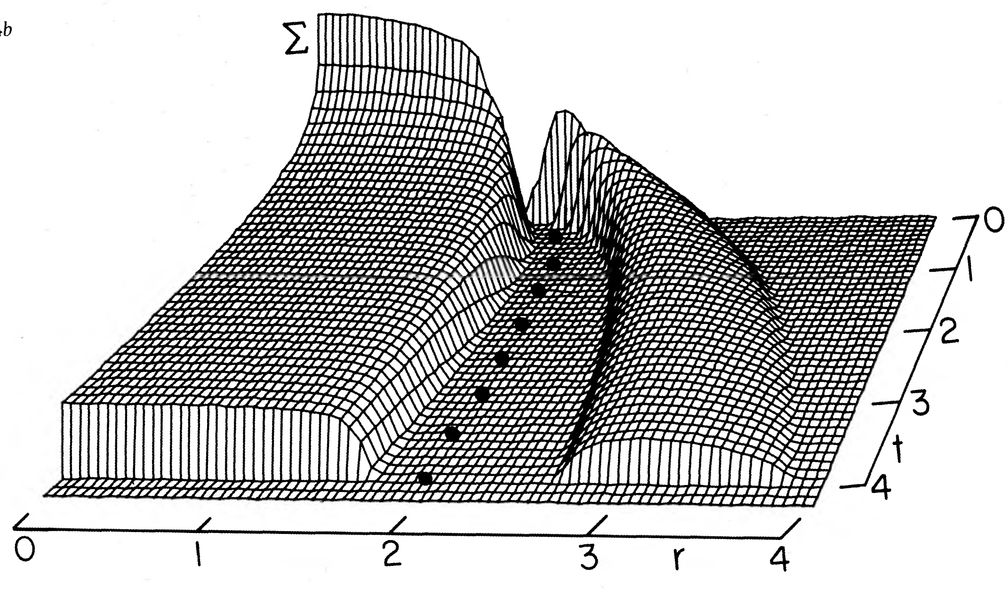

FIG. 4c

FIG. 4.—Evolution of the disk's Σ distribution and the protoplanet's orbit. For every case, $A = 10^{-3}$, $B = 20$, and $h_0 = 0.05$. Initial $r_p = (g)$ 0.6, (b) 0.7, and (c) 0.8. At $\tau = 0$, $\Sigma = 1$ for $r \leq 1$ and 0 elsewhere. The location of the protoplanet is indicated by a filled circle.

© American Astronomical Society • Provided by the NASA Astrophysics Data System

1986ApJ...309..846L

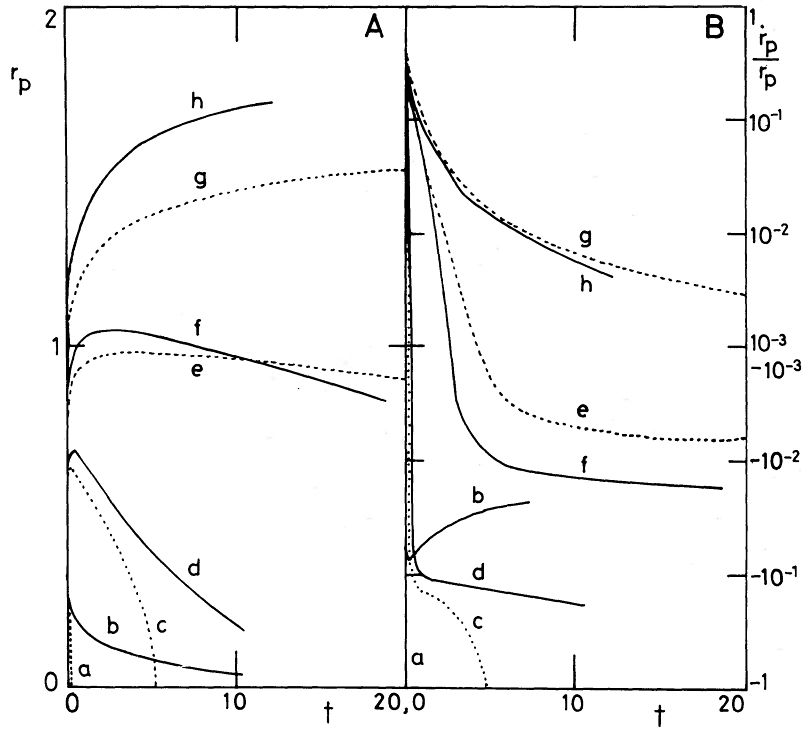

FIG. 5.—Evolution of protoplanet's orbit and analogous fluid element. The values of Σ, A, B, and h_0 are the same as in Fig. 4. The dotted curves a, c, e, and g are for fluid elements initially located at 0.4, 0.6, 0.7, and 0.8, in a freely expanding disk. The solid curves b, d, f, and h represent the orbital evolution of a protoplanet embedded in the disk which is initially located at $r_p = 0.4, 0.6, 0.7$, and 0.8 respectively (cases IXa, IXb, IXc, and IXd). (a) Evolution of position; (b) $\dot{r}_p/r_p$.

location of maximum viscous stress moves outward (Lynden-Bell and Pringle 1974). When the protoplanet's loss of angular momentum to the outer regions of the disk cannot be replenished, it migrates inward. If the protoplanet is initially located at a very large radius, it would not migrate inward until most of the disk's material is depleted (curve h).

Throughout the course of evolution, the protoplanet maintains a strong tidal coupling to the disk. This property is well illustrated by the relative position of the protoplanets and the surface density distribution (Fig. 4). Note that the position of the protoplanet is slightly closer to the inner edge of the gap. Because the surface density is slightly larger in the inner regions, dH_T/dt from each side is delicately balanced. In all cases, the surface density distribution interior to the protoplanet's orbit is approximately uniform. This distribution implies that the mass transfer rate is also uniform in that region of the disk. For $\tau \lesssim 10$, the mass transfer rate onto the origin is very similar for each case. Exterior to the protoplanet, the surface density peaks slightly outside the outer edge of the gap. Although there is no mass transfer in gap, the two regions of the disk are still dynamically connected by the tidal torque of the protoplanet.

c) *Variations from the Standard Models*

The mass ratio between the disk and the protoplanet is expressed by the parameter B. If $B \gg 1$, the protoplanet's moment of inertia is relatively small, so that the protoplanet is essentially carried along by the viscously diffusing disk. For relatively small B, the protoplanet provides a very large reservoir of angular momentum, and the evolution of the disk has little effect on the protoplanet's orbit. In Figure 6, we present the evolution of the protoplanet's orbit and the disk structure for $A = 10^{-3}$ and five values of B (0.1, 1, 5, 20, 80), for cases Xa–Xe, in curves a–e respectively. In all cases, we choose initial $r_p = 0.7$ and $h_0 = 0.05$. These results are in good agreement with our expectation. In the case where $B = 0.1$, although there is still more than half the initial mass left in the disk for $\tau \geq 10$, the protoplanet cannot migrate by any appreciable amount. In the limit that the protoplanet's mass is much smaller than that of the disk ($B = 80$), the radial extent of the orbital migration is also modest.

The above results indicate that the rate and extent of orbital migration is not very sensitive to the magnitude of B, at least for initial $r_p = 0.7$. We now consider the effect of variation in B for other initial values of r_p. In Figure 7a, we plot in curves a, b, and c the cases XIa, XIb, and XIc with initial $r_p = 0.8$, 0.7, and 0.6 respectively for $A = 10^{-3}$ and $B = 5$. In Figure 7b, we plot a similar set of initial r_p for $B = 80$ (cases XIIa, XIIb, and XIIc). These results and those presented in Figures 5 and 6 indicate that when the mass of the protoplanet is relatively large, the rate and extent of orbital migration is more sensitively dependent on the location of the protoplanet, with respect to the mass distribution of the disk, than on the magnitude of B.

The strength of the tidal forcing is proportional to A. The evolution of the disk surface density is strongly affected by the presence of the protoplanet if A is relatively large, whereas the protoplanet may not completely truncate the disk to prevent mass flow across its orbit if A is relatively small. In order to examine the dependence of r_p evolution, we consider three sets of cases each with initial $r_p = 0.7$. In cases XIIIa, XIIIb, and XIIIc, $B = 1$, and the curves a, b, and c denote $A = 5 \times 10^{-3}$, 10^{-3}, and 2×10^{-4} respectively (Fig. 8a). In cases XIVa, XIVb, and XIVc, $B = 5$ and the curves a, b, and c represent $A = 10^{-2}$, 10^{-3}, and 10^{-4} respectively (Fig. 8b). In cases XVa, XVb, and

© American Astronomical Society • Provided by the NASA Astrophysics Data System

1986ApJ...309..846L

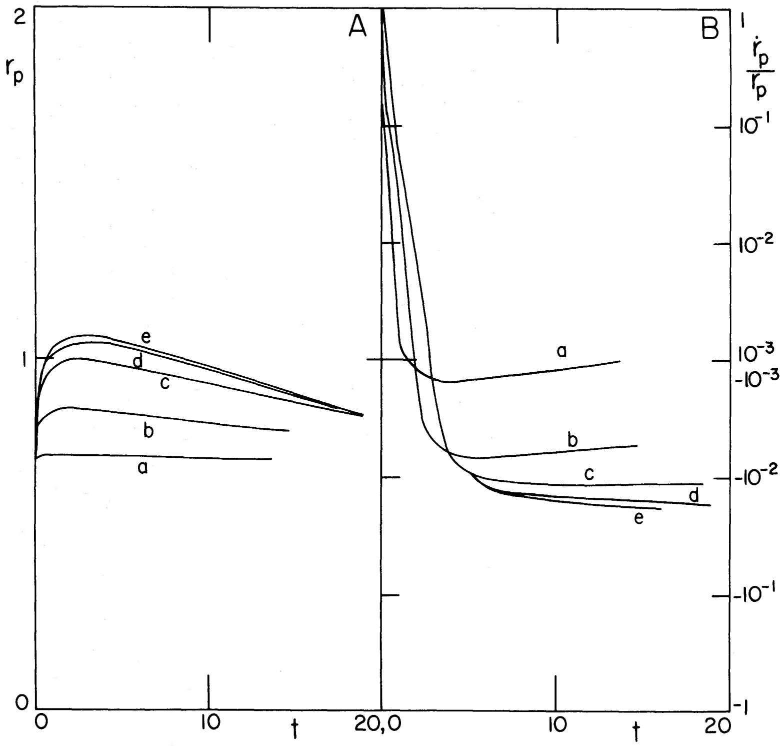

FIG. 6.—Evolution of the protoplanet and the disk for several values of B. For every case in Fig. 6, $A = 10^{-3}$. Curves a, b, c, d, and e represent cases with $B = 0.1$, 1, 5, 20, and 80 respectively (cases Xa, Xb, Xc, Xd, and Xe). The same quantities are plotted as in Figs. 5a and 5b. We also adopt the same initial Σ distribution and value for h_0.

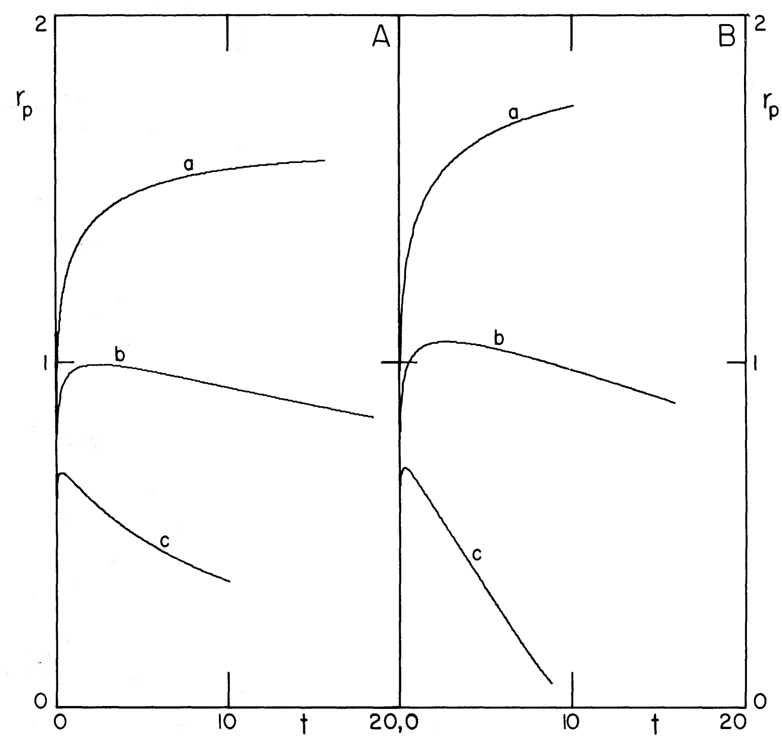

FIG. 7.—Orbital evolution of the protoplanet. (a) $A = 10^{-3}$, $B = 5$ (cases XIa, XIb, and XIc). (b) $A = 10^{-3}$, $B = 80$ (cases XIIa, XIIb, and XIIc). Curves a, b, and c are for initial $r_p = 0.8$, 0.7, and 0.6 respectively.

© American Astronomical Society • Provided by the NASA Astrophysics Data System

1986ApJ...309..846L

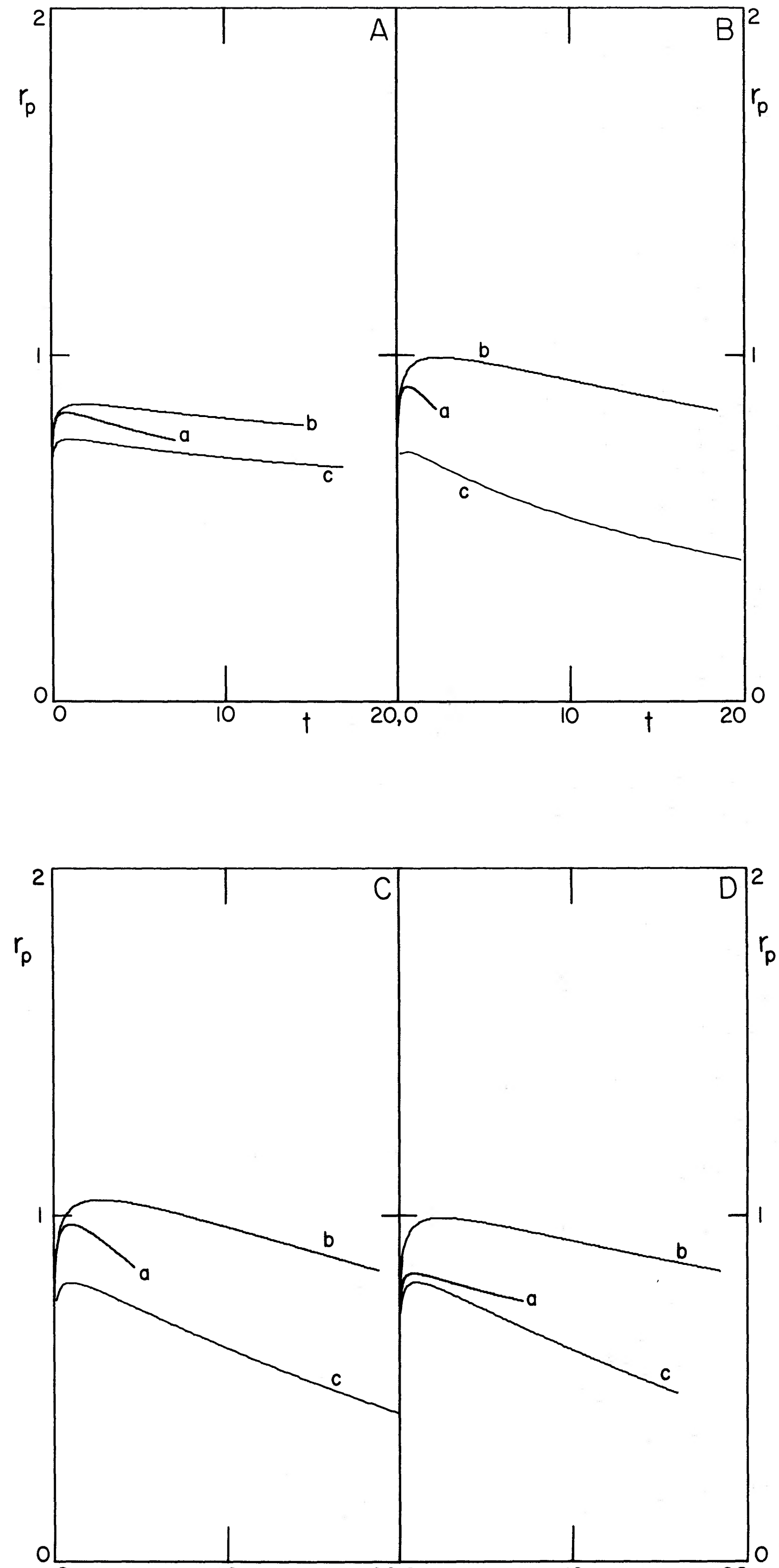

FIG. 8.—Orbital evolution of the protoplanet with $r_p = 0.7$ (*a*) $B = 1$. Curves *a*, *b*, and *c* represent the cases $A = 5 \times 10^{-3}$, 10^{-3}, 10^{-3}, and 2×10^{-4} respectively (cases XIIIa, XIIIb, and XIIIc) (*b*) $B = 5$. Curves *a*, *b*, and *c* represent the cases $A = 10^{-2}$, 10^{-3}, and 10^{-4} respectively (cases XIVa, XIVb, and XIVc). (*c*) $B = 20$ curves *a*, *b*, and *c* represent the same values of *A* as in (*a*) (cases XVa, XVb, and XVc). (*d*) Curves *a*, *b*, and *c* represent $A = 5 \times 10^{-3}$, $B = 1$; $A = 10^{-3}$, $B = 5$; and $A = 2 \times 10^{-4}$, $B = 25$ respectively (cases XVIa, XVIb, and XVIc), so that the product of *A* and *B* is 5×10^{-3} for all these cases.

© American Astronomical Society • Provided by the NASA Astrophysics Data System

1986ApJ...309..846L

XVc, $B = 20$ and the curves *a*, *b*, and *c* represent the same values of A as in case XIII (Fig. 8*c*). These results indicate that when the magnitude of A is relatively small, the sufficient condition for tidal truncation is marginally satisfied initially. The disk is not completely truncated until the disk's effective viscosity has decreased with the depletion of disk's material. After gap formation, the protoplanet's orbital evolution proceeds on time scales considerably longer than that for viscous diffusion. For relatively large A, the width of the gap is relatively large, and the protoplanet is strongly coupled to the disk. In this case, significant initial orbital evolution can occur on time scales relatively short compared with the viscous diffusion time scale.

In principle, the rate of orbital migration is independent of the magnitude of A. But in our notation, the viscous diffusion time scale is directly proportional to A. Since we are plotting r_p against the viscous diffusion time scale, the evolution for various cases of A follows a different path. Finally, in Figure 8*d*, we consider cases XVIa, XVIb, and XVIc, with the same initial r_p (0.7) and $AB = 5 \times 10^{-3}$. Curve *a* represents $A = 5 \times 10^{-3}$ and $B = 1$, curve *b* represents $A = 10^{-3}$ and $B = 5$, and curve *c* represent $A = 2 \times 10^{-4}$ and $B = 25$. According to equation (18), the orbital evolution pattern should be very similar for these three cases if the protoplanet induce a similar response from the disk. Our results indeed indicate that the overall evolutions of the disk and the protoplanetary orbit are quite similar.

VI. SUMMARY

The calculations presented above indicate: (1) the orbital migration process does not modify the condition for tidal truncation provided $t_{\rm grad} \lesssim \tau_\Delta$ or equivalently $M_p/(\Sigma_n R_p^2) \gtrsim (H_\infty/R_p)^3$. (2) When gap formation first occurs, the amount of disk material cleared to either side of the gap is determined by the motion as well as the mass of the embedded protoplanet. The disk response has a tendency to modify and local surface density gradient so that the angular momentum transfer rate between the protoplanet and the region interior to it is delicately balanced by that between the protoplanet and the disk exterior to it. (3) After a short rapidly evolving transitory phase, the protoplanet's orbital evolution proceeds on a viscous diffusion time scale, provided the mass of the protoplanet is not too large. (4) If the mass of the protoplanet is relatively large compared with that of the disk, no significant orbital evolution will take place. (5) If the protoplanet's mass is relatively small compared with that of the disk, being controlled by viscous evolution, the direction and time scale of protoplanetary orbital migration are determined by the location of the protoplanet with respect to the mass distribution of the disk. (6) If the protoplanet is initially located at small radii, it would migrate inward on a relatively short time scale, whereas if it is initally located at relatively large radii, it would migrate outward until the disk material interior to its orbit is somewhat depleted. (7) After it has truncated the disk the protoplanet cannot double its distance from the protosun unless the disk mass interior to its orbit exceeds that exterior to its orbit by a large amount. (8) Even if the protoplanet is placed on the outside of the disk, after rapidly reaching an equilibrium separation from the disk edge, further evolution occurs on the slow viscous time scale.

From the above results, we make the following conjectures: (1) Jupiter was formed outside the present radius of Mars; and (2) the disk mass exterior to Jupiter's orbit at formation did not exceed that interior to its orbit by more than 0.1 $M_\odot$; otherwise Jupiter's orbit would have evolved into the protosun in less than 10^6 yr. We also speculate that the disk mass interior to Jupiter's radius did not exceed that exterior to its orbit by 0.1 $M_\odot$, so that Jupiter's outward orbital migration did not cause some of the resonant asteroids to escape from their orbital resonances with Jupiter.

The results obtained here can be used to study the dynamics of both planetary rings and solar system formation. It may be of interest to investigate the dynamical evolution of several protoplanets in a disk. It may also be of interest to examine the possibility that there may have been, at some stage of solar system formation, a protogiant planet interior to the orbit of Jupiter that has evolved into the protosun. Finally, the results presented here may be relevant to the evolution of fragments according to the fission hypothesis. We shall consider these issues elsewhere.

We thank the directors of Lick Observatory, R. Kraft, the Canadian Institute for Theoretical Astrophysics, S. Tremaine, and the School of Mathematical Sciences, Queen Mary College, I. Roxburgh, for hospitality during part of this work. We thank P. Bodenheimer, A. G. W. Cameron, and S. Ruden for useful conversations. This work is supported in part by grants AST-83-01229 and INT-85-13479 from the NSF and NCA2-65 from NASA through the Center for the Studies of Star Formation. We also thank the staff at IBM Palo Alto Scientific Center, especially A. Karp, for assistance in allocating valuable time on the IBM 3081 computer.

REFERENCES

Bath, G., and Pringle, J. E. 1981, *M.N.R.A.S.*, **194**, 967.
Cameron, A. G. W. 1962, *Icarus*, **1**, 13.
Goldreich, P., and Tremaine, S. 1980, *Ap. J.*, **241**, 425.
———. 1982, *Ann. Rev. Astr. Ap.*, **20**, 249.
Hourigan K., and Ward, R. W. 1984, *Icarus*, **60**, 29.
Lewis, J. S. 1972, *Icarus*, **16**, 241.
———. 1974, *Science*, **186**, 440.
Lin, D. N. C. 1981, *Ap. J.*, **246**, 978.
Lin, D. N. C., and Bodenheimer, P. 1982, *Ap. J.*, **262**, 768.
Lin, D. N. C., and Papaloizou, J. 1979*a*, *M.N.R.A.S.*, **186**, 789.
———. 1979*b*, *M.N.R.A.S.*, **188**, 171.
Lin, D. N. C., and Papaloizou, J. 1980, *M.N.R.A.S.*, **191**, 37.
———. 1985, in *Protostars and Planets II*, ed. D. Black and M. Mathews (Tucson: University of Arizona Press), p. 981.
———. 1986, *Ap. J.*, **307**, 395.
Lynden-Bell, D., and Pringle, J. E. P. 1974, *M.N.R.A.S.*, **168**, 603.
Papaloizou, J., and Lin, D. N. C. 1984, *Ap. J.*, **285**, 818.
Richtmyer, R. D., and Morton, K. W. 1967, *Difference Method for Initial-Value Problems* (2d ed; New York: Wiley/Interscience).
Ruden, S., and Lin, D. N. C. 1986, *Ap. J.*, **308**, 883
Shakura, N. I., and Sunyaev, R. A. 1973, *Astr. Ap.*, **24**, 337.

D. N. C. Lin; Lick Observatory and Board of Studies in Astronomy and Astrophysics, University of California, Santa Cruz, CA 95064

John Papaloizou: School of Mathematical Sciences, Queen Mary College, Mile End Road, London E1 4NS, England

© American Astronomical Society • Provided by the NASA Astrophysics Data System